1

2

3

4

5

6 **This is the post-print version of the contribution published as:**

7

E. Padoan, F. Ajmone-Marsan, X. Querol, F. Amato

An empirical model to predict road dust emissions based on pavement and traffic characteristics

Environmental Pollution 2017

https://doi.org/10.1016/j.envpol.2017.10.115

8

9 **The publisher's version is available at:**

10

11 http://www.sciencedirect.com/science/article/pii/S0269749117332864

12

13

14 **When citing, please refer to the published version.**

15

16

17

An empirical model to predict road dust emissions based on pavement and traffic characteristics

Elio Padoan[a,b], Franco Ajmone-Marsan[a], Xavier Querol[b], Fulvio Amato[b]

[a] Dipartimento di Scienze Agrarie, Forestali e Alimentari (DISAFA), Università degli Studi di Torino, Largo Paolo Braccini 2, 10095 Grugliasco (TO), Italy
 e-mails: elio.padoan@unito.it; franco.ajmonemarsan@unito.it

[b] Institute of Environmental Assessment and Water Research (IDÆA), Spanish National Research Council (CSIC), C/ Jordi Girona 18-26, 08034 Barcelona, Spain
e-mails: xavier.querol@idaea.csic.es; fulvio.amato@idaea.csic.es

Corresponding author:

Elio Padoan

Chimica Agraria e Pedologia, Dipartimento di Scienze Agrarie, Forestali e Alimentari (DISAFA), Università degli Studi di Torino, Largo Paolo Braccini 2, 10095 Grugliasco (TO), Italy

elio.padoan@unito.it

Abstract

The relative impact of non-exhaust sources (i.e. road dust, tire wear, road wear and brake wear particles) on urban air quality is increasing. Among them, road dust resuspension has generally the highest impact on PM concentrations but its spatio-temporal variability has been rarely studied and modeled. Some recent studies attempted to observe and describe the time-variability but, as it is driven by traffic and meteorology, uncertainty remains on the seasonality of emissions. The knowledge gap on spatial variability is much wider, as several factors have been pointed out as responsible for road dust build-up: pavement characteristics, traffic intensity and speed, fleet composition, proximity to traffic lights, but also the presence of external sources. However, no parameterization is available as a function of these variables.

We investigated mobile road dust smaller than 10 µm (MF10) in two cities with different climatic and traffic conditions (Barcelona and Turin), to explore MF10 seasonal variability and the relationship between MF10 and site characteristics (pavement macrotexture, traffic intensity and proximity to braking zone). Moreover, we provide the first estimates of emission factors in the Po Valley both in summer and winter conditions. Our results showed a good inverse relationship between MF10 and macro-texture, traffic intensity and distance from the nearest braking zone. We also found a clear seasonal effect of road dust emissions, with higher emission in summer, likely due to the lower pavement moisture. These results allowed building a simple empirical mode, predicting maximal dust loadings and, consequently, emission potential, based on the aforementioned data. This model will need to be scaled for meteorological effect, using methods accounting for weather and pavement moisture. This can significantly improve bottom-up emission inventory for spatial allocation of emissions and air quality management, to select those roads with higher emissions for mitigation measures.

Keywords

PM10; non-exhaust; resuspension; macrotexture; aggregate size

Capsule

A simple empirical model, predicting maximal resuspension emission potential, was developed basing on pavement macrotexture, traffic intensity and proximity to braking zone.

81

Introduction

Particulate matter (PM) emissions from road dust resuspension are an increasing concern for air quality and public health (Denier van der Gon et al., 2013; Amato et al., 2014). The stricter PM emission standards adopted in Europe, with the EURO Directive, have brought now more attention to the non-exhaust particles from road traffic (i.e. road dust, tire wear, road wear and brake wear particles), for which emissions are not controlled, and their relative impact on urban air quality is increasing (Amato et al., 2014b; Barmadipos et al., 2012). In Southern Spain, for example, Amato et al. (2104b) found decreasing contributions for motor exhaust (p< 0.001) of 0.4 (0.57–0.24) µg m^{-3}year^{-1} from 2004 to 2011. Conversely, in the same period, road dust contributions to PM10 levels remained stable. Current estimates suggest that, in the European domain, non-exhaust vehicle emissions represent 70% of urban primary PM10 emissions since 2015 (Keunen et al., 2014). Among non-exhaust sources, road dust resuspension has generally the highest impact in PM concentrations, however, a comprehensive assessment of road dust impact both in terms of pollutants (dust, carbonaceous particles and metals) concentrations and health outcomes has been rare (Ostro et al., 2011). This is due to the lack of reliable emission factors (for source oriented models, Schaap et al., 2009), and the similarity of the chemical composition of road dust with other mineral sources (Amato et al., 2009). Moreover, experimental studies on road dust characterization generally found high variability of road dust loadings in space and time, suggesting the need of bottom-up inventories and improvement in the description of spatial and temporal variability. Spatial inequalities of air pollution levels have been in fact observed at the urban scale, mostly for PM10 and its coarser fraction, which is dominated by road dust resuspension. Time variability is crucial for epidemiological studies but information is lacking on the day-to-day and seasonal variability of emission factors. Some recent studies attempted to observe and possibly describe the spatio-temporal variability. In Scandinavian countries, the use of studded tires and road salting/sanding are predictor variables to estimate road dust loadings and the NORTRIP model has been successfully applied in order to predict both spatial and temporal variability of road dust loadings (Denby et al., 2013a and 2013b); while in Central and Southern Europe, where time-variability is driven by meteorology, in addition to traffic flow, several authors used the ON/OFF approaches to account for road moisture due to precipitation (Pay et al., 2011; Schaap et al., 2009). Amato et al. (2012) studied the day-to day variability of road dust suspendible fraction in one Spanish and one Dutch streets, observing relatively short recovery rates within 24 h and 72 h respectively, which is in agreement with the recovery of ambient air PM coarse curbside increment (Amato et al., 2011; Keuken et al., 2010). However, uncertainty remains on the seasonal variability of road dust emissions, which can be also affected by meteorological pattern (higher relative humidity in winter, higher drought in summer, intense Saharan dust intrusions in spring, for example). Concerning the spatial variability, the gap of knowledge is much wider. Several factors have been pointed out as responsible of road dust build-up (i.e. emission potential): pavement characteristics (texture, mineralogy, age (Amato et al., 2013; Denby et al., 2013b; China and James, 2012; Berger and Denby, 2011; Gehrig et al., 2010; Gustafsson et al., 209; Raisanen et al., 2005), traffic intensity and speed, fleet composition (Bukowiecki et al., 2010; Liu et al., 2016), proximity to traffic lights,

118 but also the presence of external sources (e.g. construction dust, unpaved areas, African dust deposition, etc.).

119 However, no parameterization is available as a function of these variables. Moreover, to understand the impact

120 of these predictors is also important for air quality management since remediation measures can be designed.

121 In this study, we present a simple empirical model able to predict road dust suspendible fraction and,

122 consequently, emission potential, based on pavement macrotexture, traffic intensity and proximity to braking

123 zone. This model is based on field measurement in the cities of Turin (Italy) and Barcelona (Spain), thus

124 considering quite contrasting environments (Mediterranean and Continental) and aims to estimate the

125 maximum emission factor for single roads (without considering the effect of meteorology); it could be,

126 therefore, suitable for spatial allocation of emissions. Moreover, the article offers the first estimates of emission

127 factors in the Po Valley (Italy), one of the most polluted regions in Europe, both in summer and winter

128 conditions.

129

130 **Methods**

131 *Study area*

132 Four sampling campaigns were performed in the cities of Turin (Italy) and Barcelona (Spain), three in the

133 summer period (June and September 2016 in Turin, August 2016 in Barcelona) and one in winter (January

134 2017, in Turin). The two cities under study have a common high density of vehicle emissions (among the

135 highest in Europe) but different climatic conditions.

136 The Turin metropolitan area has a population of around 1.5 million inhabitants, and is the fourth most populous

137 metropolitan area in Italy. The high car density (5300 veh km^{-2}) provokes (as sum of exhaust and non-exhaust)

138 almost 40% of the total primary emitted PM10, the second most important source (after biomass burning),

139 according to the regional inventory (IREA, 2010). Climate is classified as humid subtropical, with moderately

140 cold but dry winters and hot summers, when rains are infrequent but heavy. Average rainfall is around 1000

141 mm per year (mostly concentrated in spring and autumn) and daily temperatures vary within 2-22 °C (monthly

142 averaged; ARPA Piemonte, 2014). The city is located at the western end of the Po valley, surrounded by hills

143 to the East and by the Alps to the North and West. Thus, the dispersion of pollutants is very low, as in all cities

144 of the Po valley (Eeftens et al., 2012; Belis et al., 2011), due to the very low wind speed and the thermal

145 inversion occurring in wintertime. Consequently, EC air quality standards are not met. In 2016, for example,

146 PM10 concentrations in the city center exceeded the EU daily limit value for 70 days (ARPA Piemonte, 2016).

147 The Barcelona greater metropolitan area has around 4 million inhabitants and, with ~1 million vehicles, has

148 also one of the highest car densities in Europe (5900 veh km^{-2}). The city is located in the western coast of the

149 Mediterranean basin, with a Mediterranean climate (mild winter and hot summers), and the scarce and

150 infrequent precipitation (614 mm as mean from 2010 to 2015) facilitate the mobilization and resuspension of

151 road-deposited particles. In Barcelona, traffic emissions are the most important pollution source of PM10,

152 although other significant sources are mineral dust, shipping and industry (Amato et al., 2016). At urban

153 background sites, annual PM10 concentrations due to the regional contribution are less than 30% of the total,

154 while non-exhaust vehicle emissions contribute 17% (7 mg m^{-3}), with the total road traffic contribution

5

155 calculated at 46% (Amato et al., 2009). Thus, controlling local sources is very important for attaining PM10

156 limit values. The exposure scenario is even more problematic considering that 56% of urban population live

157 less than 70 m away from major roads (>10,000 vehicles day^{-1}).

158

159 *Road dust sampling*

160 The mobile fraction (able to be suspended under the applied airflow, 30 l min^{-1}) of road dust below <10 µm in

161 aerodynamic diameter (MF10) was sampled by means of a field dry resuspension chamber consisting in a

162 sampling tube, a methacrylate deposition chamber, an elutriation filter, where MF10 was separated, and a filter

163 holder, where particles were collected (a picture is available in Supplementary Material, Figure SM1). More

164 details on the sampler can be found in Amato et al. (2009; 2011).

165 In Turin, sampling sites were selected in order to characterize different fleet conditions, pavements and traffic

166 characteristics. To this aim, sites were chosen in residential, commercial and industrial neighborhoods and, at

167 some sites, sampling was performed in both traffic directions. In Barcelona, sampling sites were chosen in a

168 limited area, but on streets with different pavements and traffic conditions. In total, 72 filters were collected,

169 characterizing 30 sites in Turin and 6 sites in Barcelona (a map of sampling sites is reported in Figure SM2).

170 In order to ensure a complete re-establishment of the stationary conditions of dust loadings, all the samplings

171 were performed after, at least, one week without precipitation.

172 Each MF10 sample was collected as in previous studies, from a 50 x 100 cm area with the wider side centered

173 within the most-right active lane (excluding parking area), thus representing the area covered by wheel tracks

174 (Figure 1). For each site 2 filters were collected in adjacent areas to improve the representativeness of the final

175 road dust loading estimate.

176 Before sampling, quartz fiber filters (Pall, Ø47 mm) were dried at 205°C for 5 h and conditioned for 48 h at

177 20°C and 50% relative humidity. Blank filters were weighed three times every 24 h and kept in PETRI holders.

178 After sampling, filters were brought back to the laboratory and weighted after 24 and 48 h of conditioning at

179 the same T and HR condition.

180

181 *Pavement macro-texture measurements*

182 The macro-texture of road pavement corresponds to the size of the aggregate particles and the gaps between

183 them in the asphalt mixture (Henry, 2000). In our study, pavement macro-texture was characterized through

184 the combination of photographic analysis and the Mean Texture Depth (MTD) analysis (China and James,

185 2012). Pictures of the pavement surfaces were taken at a fixed distance using a 16.1 MP camera, with a

186 millimeter scale ruler in the field of view, and used to estimate average size of aggregates. In each site, two

187 photos were taken and the size distribution and mean horizontal size of aggregates was estimated by counting

188 the total number and the size of each aggregate along the ruler (Amato et al., 2013).

Since aggregates are embedded in the asphalt binder, the texture was estimated also by means of a MTD analysis. This analysis, called sand patch method (China and James, 2012; Praticò and Vaiana, 2015), is a standard evaluation of the surface macrostructure by careful application of a known volume of standard material on the surface, and subsequent measurement of the total area covered (ASTM E 965, 2015). At each site, two MTD measurements were made using 30 ml of glass spheres (clean silica sand passing a 300 µm and retained on a 150 µm BS sieve, Mastrad ltd) and the average circular area was calculated using the average of 3 diameter measurements. This area was then divided by the applied volume of the spheres to calculate the MTD.

The area used for photographic and MTD measurements was within the area of the MF10 measurement (Figure 1), and performed after the MF10 sampling and after sweeping the surface with a brush. Using these analyses, we calculated the corrected aggregate mode (CAM) according to the formula proposed by China and James (2012):

$$(CAM)_i = MTD_i * (aggregate\ mode)_i / (aggregate\ mean)_i \qquad (1)$$

where the CAM of the i-th sample is calculated starting from the MTD, the mode of the aggregates observed through photographic analysis and the mean value of the horizontal size of the aggregates.

Data analysis

Multiple linear regression analysis was run to assess the feasibility of using pavement and site features to predict MF10. As predictor variables, we used the corrected aggregate mode (CAM), the traffic intensity (TR) and the distance (DIST) from the closest braking zone. The method was cross-validated using the leave-one-out method (Todeschini, 1998). The indices used to interpret the validity of the model were the Relative Prediction Error (RPE) the Standard Error of Cross-Validation (SECV) and the Cross-Validated Coefficient of Determination (Q^2) (Gunawardena et al., 2014).

Regression curves have been calculated by means of a least squares fit, minimizing the sum of residuals scaled by the standard deviation among duplicated measurements. All calculations were performed using Windows Excel 2013 and IBM SPSS 23.

Data on traffic intensity was provided by the city council for Barcelona and, for Torino, by the in-house company of the city (5T s.r.l.), refers to the monthly averaged daily fluxes in the sampled month. DIST was calculated from the sampling site to the stop sign (or the traffic light line on the pavement).

Results and Discussion

MF10 loadings and emission factors

Descriptions of the sampling sites, macro-texture, traffic data, MF10 and emission factors for each site are reported in Table 1. The MF10 loadings (the suspendible fraction of road dust) in Turin streets ranged between

223   0.8 – 42.7 mg m^{-2}, being the highest three registered at sites next to unpaved parks (12.3 mg m^{-2}) and

224   construction works (11.5 and 42.7 mg m^{-2}). Excluding these sites, the urban range was found to be 0.8-8.8 mg

225   m^{-2} (mean of 2.0 mg m^{-2}) which is in the central range of European cities characterized with the same

226   methodology (Amato et al., 2011; 2012; 2014, 2016; AIRUSE, 2016) but higher than other Central European

227   cities such as Paris (0.7-2.2), and Zurich (0.7-1.3). However, Turin measurements include summer and winter

228   data, while in Zurich and Paris measurements were only performed in winter. In fact, we observed a clear

229   difference between summer and winter samples (Figure 2), with a mean winter value of 1.0 mg m^{-2},

230   significantly lower than in summer (2.7 mg m^{-2}). In Barcelona, summer MF10 loadings were found in the

231   range of 1.1 – 3.4 mg m^{-2}, confirming the values found in previous studies (Amato et al., 2012).

232   Road dust emission factors (EFs) were estimated based on MF10 using the power relationship proposed by

233   Amato et al. (2011), which has a similar theoretical basis of the USEPA AP-42 model but uses the MF10

234   instead of the silt (<75 µm) loading:

235   $$EF_i \ [mg \ VKT] = a \cdot MF10_i{}^b \qquad (2)$$

236   where MF10$_i$ is the road dust suspendible fraction at the ith location, and *a* and *b* are empirically determined

237   coefficients. In the case of Barcelona sites, we used the coefficients (a=52.9; b=0.82) obtained in the same city

238   by Amato et al. (2012), while for Turin we used the average (a=45.9; b=0.81) between Barcelona and Zurich

239   due to the climatic conditions of Turin. Emission factors for each site are reported in Table 1 and must be

240   intended as fleet-averaged.

241   Typical urban roads in Turin showed annual-averaged values within 10 – 85 mg VKT^{-1} (VKT: Vehicle

242   Kilometer Traveled, Table 1), with a mean value of 27±19 mg VKT^{-1} (excluding the sites influenced by

243   construction works or unpaved areas nearby), which is the first estimate in the Po Valley and, to our knowledge,

244   the first annual-averaged value in Europe (accounting also for seasonal differences). Separating winter and

245   summer EFs the averages would be 20±8 and 31±16 mg VKT^{-1}, respectively, although not all sites were

246   sampled at the same spot both in summer and in winter (Figure 2). An explanation for this higher emission

247   factor in summer could be the lower pavement moisture, as all winter measurements were performed under

248   morning haze and high air humidity. In addition, road hygroscopicity could have been increased by road

249   salting, although only some roads were salted the week before the sampling campaign. Unfortunately, we do

250   not have any precise information on this operation (it was made at least two days before the sampling).

251   Moreover, other unknown dust sources, such as a higher soil contribution due to the drier climate, or

252   construction dust could have influenced the results.

253   In Barcelona, emission factors were estimated within 13 – 34 mg VKT^{-1}, with an average value of 20±8 mg

254   VKT^{-1} (Table 1). If we compare our results with the emission factors estimated in European studies using the

255   same experimental set-up, these values are in the central (for Turin) or lower observed range. For example,

256   studies reported 5.4-17 mg VKT^{-1} in Paris (Amato et al., 2016), 12-51 mg VKT^{-1} in Switzerland (Amato et al.,

257   2012) and 77-480 mg VKT^{-1} in southern Spain (Amato et al., 2013).

258

Effect of traffic intensity and distance from braking zones

The impact of traffic intensity on the road dust EF is poorly known although important for improving the emission parameterization for modelling. Recent studies found or hypothesized lower EFs for high capacity roads, as high traffic intensity and speed are both expected to lead to a lower road dust reservoir (Schaap et al., 2009; Amato et al. 2013; Abu-Allaban et al., 2003; Etyemezian et al., 2003). Conversely, Bukowiecki et al., (2010) found the opposite, comparing the city center with a major freeway, revealing the need of more empirical studies. In the present study, we have explored the relationship between MF10 and street characteristics, such as traffic intensity and the distance from nearest braking zone (crossing, traffic light or roundabout), using combined data of both cities to enhance the representativeness of the models. We used traffic intensity data provided by city councils, based either on measurements or on mobility models. We observed a rather good inverse correlation between MF10 and the number of vehicles circulating on the lane (Figure 3), obtained by dividing the total traffic volume by the number of lanes. MF10 decreases with increasing traffic intensity following a power law fit, reaching a background loading probably related to pavement characteristics and meteorological conditions. In Figure 3, we have separated summer and winter samples in order to avoid the meteorological disturbance on the goodness of the fitting. Below 1000 vehicles day^{-1} MF10 increased due to lower traffic volumes, that led to higher steady state MF10 than at high traffic sites. However, also unknown sources could have contributed to the additional load, such as construction dust, due to the poor state of the pavement (at some sites). Emission factors for secondary roads were therefore higher than for high capacity roads. This finding is relevant for emission inventories, since using a single or constant emission factor for the calculation of non-exahust contribution to PM in a whole region (top-down approach), may result in a mistake in emission estimates (Figure 4), e.g emissions from road with higher intensity would be overestimated. The use of real or modeled EFs (as the site-specific relation in Figure 4) for each road or area (bottom-up approach) for road dust emissions is therefore needed to improve modeling results.

Brake wear particles are a major source of road dust (Grigoratos and Martini, 2015; Thorpe and Harrison, 2008). In Barcelona, Amato et al. (2013) estimated that 27% of MF10 was made of brake wear, as traced by Cu, Sb, Ba among other elements. Therefore, we explored the relationship between MF10 and proximity to braking zone (Figure 5) as a possible predictor of MF10 loading. We explored the relationship with the distance both to the following braking zone and to the previous, or the smaller of the two. Results reported in Figure 5 show a rather poor correlation in the case of using the minimum distance but a negative trend is apparent, suggesting that 70-100 m away from braking zone no significant increase in MF10 is observed due to brake particles. These results are in agreement with Hagino et al. (2015), who found two peaks of brake PM emission in dynamometer tests: the first peak during the application of a braking force and the second one afterwards, during wheel rotation. In one case, the peak was even after 30 s of acceleration, thus after a considerable space in the real world, and the emission during the acceleration phase represented almost 50% of the emitted PM.

Effect of macro-texture

296   In this study macro-texture was investigated through MTD and photographic measurements in order to

297   calculate CAM values. The classic MTD measurement typically resulted in a value indicating the mean size

298   of the gaps between aggregate particles, thus higher MTDs indicated deeper or larger pores (coarser texture),

299   while the CAM value also incorporated an estimation of the horizontal size of the particles.

300   MTD values ranged from 0.56 to 1.30 mm in Turin, and from 0.36 to 1.54 mm in Barcelona (Table 1), showing

301   quite a large variability in pavement macro-texture. Figure 6 shows the relationship between MF10 and both

302   the MTD and the CAM, using data of both cities but excluding roads with less than 1000 vehicles day^{-1}, where,

303   as described above, unknown sources could have contributed to the high loadings. In addition, in these streets

304   the traffic data was only modeled and not measured as in all other sites, thus introducing an additional error.

305   Results show a significant inverse correlation with both parameters (r^2= 0.48 and 0.54 for MTD and CAM,

306   respectively). The correlation is higher with the corrected aggregate mode (Figure 6), revealing that the higher

307   the porosity of asphalt, the higher the capability to inhibit resuspension. A similar result was found by China

308   and James (2012), who analyzed the relationship of mean corrected mode with the resuspension potential using

309   standard soil freshly applied to asphalt, and by Gehrig et al. (2010), using mobile load simulators. Moreover,

310   Jacobson and Wågberg (2007) found that, with studded tires, the aggregate diameter of the pavements

311   influences the total wear in as much as coarser material results in lower wear. However, those studies were

312   both dealing with controlled experiments, which might not be fully applicable to the real world, while our

313   study offers the first evidence, to our knowledge, in real-world conditions (regarding road dust loading and

314   physico-chemical properties). The resuspension inhibition could be influenced by the physical shielding of

315   pores and by the size distribution of particles in the bitumen matrix, as evidenced by the improvement of the

316   fit using the CAM. This improvement could be attributed to the use of the ratio of mode to mean (in equation

317   1). A value lower than 1 means that some large particles are enclosed in the matrix, so dust could be occluded

318   between these particles and the pavement or sheltered from them, causing a higher build-up or road dust. On

319   the other hand, if we have a number of particles finer than the average, they can smooth or occlude the pores

320   between larger particles, thus lowering the dust accumulation potential. Still, it must bear in mind that this

321   relationship is only valid in summer, being completely masked in winter by the stronger effect of road moisture

322   (Figure 6).

323   Recently, review studies on non-exhaust emissions (Denier van der Gon et al., 2013; Amato et al., 2014) have

324   suggested the possibility of the use asphalt with coarser texture to improve air quality by inhibiting road dust

325   resuspension, and our study offer experimental evidence, covering two different urban scenarios. Given that

326   the observed range of MTD variability is high (Table 1), even within the same urban area, there is space for

327   improvement since, currently, the surface texture is not regulated in cities. These results suggest that asphalts

328   that are more porous and with coarser textures could, therefore, be not only designed to reduce noise emissions

329   and to improve water drainage, but also to reduce the emissions from paved roads.

330

331   *Predicting model*

332 Our predicting model aims to estimate MF10 loading contributions from traffic sources, not from external

333 sources (e.g. construction dust, soil resuspension or African deposition). Therefore, only the spatial variability

334 could be assessed, as the temporal variability needs to be parametrized afterwards, using, for example, the

335 method proposed by Amato et al. (2012).

336 Based on the results and the relationships discussed above, a multiple linear regression analysis was developed

337 to predict the maximum MF10 loading from the CAM, the traffic intensity (TR) and the distance (DIST) from

338 the closest braking zone. Independently, each parameter showed an inverse relationship with the MF10, thus

339 we tried different linear regressions with two or three variables using exponential or potential equations. Our

340 results show that the equation with the best prediction of MF10 was:

341 $$RD10 = e^{2.901 \pm 0.855} \times CAM^{-0.264 \pm 0.123} \times TR^{-0.218 \pm 0.105} \times DIST^{-0.145 \pm 0.076} \qquad (3)$$

342 The model performed well, reporting the 74% of the variance of the dataset and reported no systematical bias

343 in calculated values (Figure 7). During the development, we removed from the dataset samples below 1000

344 vehicles day^{-1}, for the above-depicted rationale, and samples where not all the data were available.

345 The validation of the method (performed with the leave-one-out method due to the low number of samples)

346 gave also encouraging results, with an RPE value of 22% and a cross-validated coefficient of determination

347 (Q^2) of 0.65, that indicate a good fit of the data. To have a better idea of the fit maintaining the original data

348 scale, the cross-validated standard error (SECV) was 0.52 mg m^{-2}. Converted as an error on emission factors,

349 it corresponds to 7 mg VKT^{-1}, a very encouraging result on maxima emission potentials, as we started from

350 mostly non-parametrized or city-averaged inventories.

351 Our model can be therefore used for predicting road dust loadings for multiple objectives: bottom-up emission

352 inventory, road maintenance for air quality management and air quality measures in general.

353

Conclusions

355 In this study, we explored the influence of road characteristics such as pavement macro-texture, traffic intensity

356 and distance to braking zones on real-world road dust loading that can be mobilized and resuspended (i.e.

357 emission factor) in two contrasting environments such as the cities of Turin and Barcelona. Our results showed

358 good inverse relationship between MF10 and i) macro-texture, ii) traffic intensity and iii) distance from

359 braking zone, although with a lower correlation. These results allowed building an empirical mode, able to

360 predict suspendable road dust and emission factors based on the aforementioned road data. This model can

361 significantly improve bottom-up emission inventory for spatial allocation of emissions and air quality

362 management to select those roads with higher emissions for mitigation measures. We also found a clear

363 seasonal effect of road dust emissions, with higher emission in summer likely due to the lower pavement

364 moisture, indicating that our model could be used only for predicting spatial variability of maxima emissions,

365 which then need to be scaled for meteorological effect, using methods accounting for weather and pavement

366 moisture.

373

374 **References**

375 Abu-Allaban, M., Gillies, J.A., Gertler, A.W., Clayton, R., Proffitt, D., 2003. Tailpipe, resuspended road dust,
376 and brake-wear emission factors from on-road vehicles. Atmospheric Environment 37 (37), 5283-
377 5293. http://doi.org/10.1016/j.atmosenv.2003.05.005

378 AIRUSE LIFE 11 ENV/ES/584, PM10 trends in the AIRUSE cities, Action B1, February 2015,
379 http://airuse.eu/wp-content/uploads/2013/11/R03_AIRUSE-PM10-trends-in-AIRUSE-cities.pdf
380 (accessed December 12, 2016)

381 Amato, F., Pandolfi, M., Viana, M., Querol, X., Alastuey, A., Moreno, T., 2009. Spatial and chemical patterns
382 of PM10 in road dust deposited in urban environment. Atmos. Environ. 43, 1650–1659.
383 http://doi.org/10.1016/j.atmosenv.2008.12.009

384 Amato, F., Nava, S., Lucarelli, F., Querol, X., Alastuey, A., Baldasano, J., Pandolfi, M., 2010. A
385 comprehensive assessment of PM emissions from paved roads: real-world emission factors and intense
386 street cleaning trials. Sci. Total Environ. 408, 4309-4318.
387 http://doi.org/10.1016/j.scitotenv.2010.06.008

388 Amato, F., Pandolfi, M., Moreno, T., Furger, M., Pey, J., Alastuey, A., Bukowiecki, N., Prevot, A.S.H.,
389 Baltensperger, U., Querol, X., 2011. Sources and variability of inhalable road dust particles in three
390 European cities. Atmos. Environ. 45, 6777–6787. http://doi.org/10.1016/j.atmosenv.2011.06.003

391 Amato, F., Schaap, M., Gon, H.A.C.D. van der, Pandolfi, M., Alastuey, A., Keuken, M., Querol, X., 2012.
392 Effect of rain events on the mobility of road dust load in two Dutch and Spanish roads. Atmos. Environ.
393 62, 352–358. http://doi.org/10.1016/j.atmosenv.2012.08.042

394 Amato, F., Pandolfi, M., Alastuey, A., Lozano, A., Contreras González, J., Querol, X., 2013. Impact of traffic
395 intensity and pavement aggregate size on road dust particles loading. Atmos. Environ. 77, 711–717.
396 http://doi.org/10.1016/j.atmosenv.2013.05.020

397 Amato, Fulvio, Cassee, F. R., Denier van der Gon, H. A. C., Gehrig, R., Gustafsson, M., Hafner, W., … Querol,
398 X., 2014. Urban air quality: The challenge of traffic non-exhaust emissions. Journal of Hazardous
399 Materials, 275, 31–36. http://doi.org/10.1016/j.jhazmat.2014.04.053

400 Amato, F., Alastuey, A., de la Rosa, J., Gonzalez-Castanedo, Y., Sánchez de la Campa, A.M., Pandolfi, M.,
401 Lozano, A., Contreras González, J., Querol, X., 2014b. Trends of road dust emissions contributions
402 on ambient air particulate levels at rural, urban and industrial sites in southern Spain. Atmospheric
403 Chemistry and Physics, 14, 3533-3544. https://doi.org/10.5194/acp-14-3533-2014, 2014

404 Amato, F., Favez, O., Pandolfi, M., Alastuey, A., Querol, X., Moukhtar, S., Bruge, B., Verlhac, S., Orza,
405 J.A.G., Bonnaire, N., Le Priol, T., Petit, J.-F., Sciare, J., 2016. Traffic induced particle resuspension
406 in Paris: Emission factors and source contributions. Atmospheric Environment 129, 114–124.
407 http://doi.org/10.1016/j.atmosenv.2016.01.022

408 ARPA Piemonte, 2014. Relazione sullo stato dell'ambiente in Piemonte,
409 http://relazione.ambiente.piemonte.gov.it/2014/it (accessed July 06, 2017).

410 ARPA Piemonte, 2016. Uno sguardo all'aria, relazione annuale sui dati rilevati dalla rete metropolitana di
411 monitoraggio della qualità dell'aria.
412 http://www.arpa.piemonte.gov.it/approfondimenti/territorio/torino/aria/Pubblicazioni/uno-sguardo-
413 allaria-2016-anteprima (accessed July 06, 2017).

414 ASTM E965-15, 2015. Standard Test Method for Measuring Pavement Macrotexture Depth Using a
415 Volumetric Technique, ASTM International, West Conshohocken, PA. http://doi.org/10.1520/E0965-
416 15

Barmpadimos, I., Keller, J., Oderbolz, D., Hueglin, C., & Prévôt, A. S. H., 2012. One decade of parallel fine (PM 2.5) and coarse (PM 10-PM 2.5) particulate matter measurements in Europe: Trends and variability. Atmospheric Chemistry and Physics, 12(7), 3189–3203. https://doi.org/10.5194/acp-12-3189-2012

Belis, C.A., Cancelinha, J., Duane, M., Forcina, V., Pedroni, V., Passarella, R., Tanet, G., Douglas, K., Piazzalunga, A., Bolzacchini, E., Sangiorgi, G., Perrone, M.G., Ferrero, L., Fermo, P., Larsen, B.R., 2011. Sources for PM air pollution in the Po Plain, Italy: I. Critical comparison of methods for estimating biomass burning contributions to benzo(a)pyrene. Atmospheric Environment 45, 7266-7275. http://doi.org/ 10.1016/j.atmosenv.2011.08.061

Berger, J., Denby, B., 2011. A generalised model for traffic induced road dust emissions. Model description and evaluation. Atmospheric Environment 45 (22), 3692-3703.

Bukowiecki, N., Lienemann, P., Hill, M., Furger, M., Richard, A., Amato, F., Prévôt, A.S.H., Baltensperger, U., Buchmann, B., Gehrig, R., 2010. PM10 emission factors for non-exhaust particles generated by road traffic in an urban street canyon and along a freeway in Switzerland. Atmos. Environ. 44, 2330–2340. http://doi.org/10.1016/j.atmosenv.2010.03.039

China, S., James, D.E., 2012. Influence of pavement macrotexture on PM10 emissions from paved roads: A controlled study. Atmos. Environ. 63, 313–326. http://doi.org/10.1016/j.atmosenv.2012.09.018

Denby, B.R., Sundvor, I., Johansson, C., Pirjola, L., Ketzel, M., Norman, M., Kupiainen, K., Gustafsson, M., Blomqvist, G., Kauhaniemi, M., Omstedt, G., 2013a. A coupled road dust and surface moisture model to predict non-exhaust road traffic induced particle emissions (NORTRIP). Part 2: Surface moisture and salt impact modelling. Atmospheric Environment 81, 485-503.

Denby, B.R., Sundvor, I., Johansson, C., Pirjola, L., Ketzel, M., Norman, M., Kupiainen, K., Gustafsson, M., Blomqvist, G., Omstedt, G., 2013b. A coupled road dust and surface moisture model to predict non-exhaust road traffic induced particle emissions (NORTRIP). Part 1: Road dust loading and suspension modelling. Atmospheric Environment 77, 283-300.

Denier van der Gon, H. A. C., Gerlofs-Nijland, M. E., Gehrig, R., Gustafsson, M., Janssen, N., Harrison, R. M., … Cassee, F. R., 2013. The Policy Relevance of Wear Emissions from Road Transport, Now and in the Future—An International Workshop Report and Consensus Statement. Journal of the Air & Waste Management Association, 63(2), 136–149. https://doi.org/10.1080/10962247.2012.741055

Eeftens, M., Tsai, M., Ampee, C., Anwanderf, B., Beelen, R., et al., 2012. Spatial variation of PM2.5, PM10, PM2.5 absorbance and PM coarse concentrations between and within 20 European study areas and the relationship with NO2 – results of the ESCAPE project. Atmos. Environ. 62:303–317. http://doi.org/10.1016/j.atmosenv.2012.08.038.

Etyemezian, V., Kuhns, H., Gilles, J., Chow, J., Hendrickson, K., McGown, M., Pitchford, M., 2003. Vehicle-based road dust emission measurement: III effect of speed, traffic volume, location and season on PM10 road dust emission in the Treasure Valley, ID. Atmospheric Environment 37, 4583-4593. https://doi.org/10.1016/S1352-2310(03)00530-2

Gehrig, R., Hill, M., Buchmann, B., Imhof, D.,Weingartner, E., Baltensperger, U., 2004. Separate determination of PM10 emission factors of road traffic for tailpipe emissions and emissions from abrasion and resuspension processes. International Journal of Environment and Pollution 22 (3), 312-325.

Gehrig, R., Zeyer, K., Bukowiecki, N., Lienemann, P., Poulikakos, L.D., Furger, M., Buchmann, B., 2010. Mobile load simulators – A tool to distinguish between the emissions due to abrasion and resuspension of PM10 from road surfaces. Atmospheric Environment 44, 4937–4943. https://doi.org/10.1016/j.atmosenv.2010.08.020

Grigoratos, T., Martini, G., 2015. Brake wear particle emissions: a review. Environmental Science and Pollution Research 22, 2491–2504. https://doi.org/10.1007/s11356-014-3696-8.

Gunawardena J., Ziyath A.M., Egodawatta P., Ayoko G.A., Goonetilleke A., 2014. Mathematical relationships for metal build-up on urban road surfaces based on traffic and land use characteristics. Chemosphere, 99, 267-271. https://doi.org/10.1016/j.chemosphere.2013.10.068

Gustafsson M, Blomqvist G, Gudmundsson A, Dahl A, Jonsson P, Swietlicki E., 2009. Factors influencing PM10 emissions from road pavement wear. Atmospheric Environment 43, 4699-4702. https://doi.org/10.1016/j.atmosenv.2008.04.028

Hagino, H., Oyama, M., Sasaki, S., 2016. Laboratory testing of airborne brake wear particle emissions using a dynamometer system under urban city driving cycles. Atmospheric Environment 131, 269–278. https://doi.org/10.1016/j.atmosenv.2016.02.014

473 Henry, J.J., 2000. NCHRP Synthesis 291, Evaluation of Pavement Friction Characteristics, TRB. National
474   Research Council, Washington, DC.
475 IREA, Inventario Regionale delle Emissioni in Atmosfera, 2010,
476   http://www.sistemapiemonte.it/fedwinemar/elenco.jsp (accessed July 14, 2017)
477 Jacobson T, Wågberg L., 2007. Developing and Upgrading of a Prediction Model of Wear Caused by Studded
478   Tyres and an Overview of the Knowledge of the Factors Influencing the Wear. VTI report 7. Swedish
479   National Road and Transport Research Institute, Linköping, Sweden. (In Swedish)
480 Ketzel M., Omstedt G., Johansson C., During I., Pohjola M., Oettl D., Gidhagen L., ... Berkowicz R., 2007.
481   Estimation and validation of PM2.5/PM10 exhaust and non-exhaust emission factors for practical
482   street pollution modelling. Atmospheric Environment, 41 (40), 9370-9385.
483   https://doi.org/10.1016/j.atmosenv.2007.09.005
484 Keuken M., Denier van der Gon H., van der Valk K., 2010. Non-exhaust emissions of PM and the efficiency
485   of emission reduction by road sweeping and washing in the Netherlands. Science of the Total
486   Environment, 408 (20), 4591-4599. https://doi.org/10.1016/j.scitotenv.2010.06.052
487 Kuenen, J. J. P., Visschedijk, A. J. H., Jozwicka, M., Denier van der Gon H. A. C., 2014. TNO-MACC_II
488   emission inventory; a multi-year (2003–2009) consistent high-resolution European emission inventory
489   for air quality modeling. Atmospheric Chemistry and Physics 14, 10963–10976.
490   https://doi.org/10.5194/acp-14-10963-2014
491 Liu, A., Gunawardana, C., Gunawardena, J., Egodawatta, P., Ayoko, G.A., Goonetilleke, A., 2016. Taxonomy
492   of factors which influence heavy metal build-up on urban road surfaces. Journal of Hazardous
493   Materials 310, 20–29. https://doi.org/10.1016/j.jhazmat.2016.02.026
494 Ostro, B., Tobias, A., Querol, X., Alastuey, A., Amato, F., Pey, J., Pérez, N., Sunyer, J., 2011. The effects of
495   particulate matter sources on daily mortality: A case-crossover study of Barcelona, Spain.
496   Environmental Health Perspectives, 119(12), 1781-1787. https://doi.org/10.1289/ehp.1103618
497 Padoan, E., Malandrino, M., Giacomino, A., Grosa, M.M., Lollobrigida, F., Martini, S., Abollino, O., 2016.
498   Spatial distribution and potential sources of trace elements in PM10 monitored in urban and rural sites
499   of Piedmont Region. Chemosphere 145, 495–507. https://doi.org/10.1016/j.chemosphere.2015.11.094
500 Pay, M.T., Jimenez-Guerrero, P., Baldasano, J.M., 2011. Implementation of resuspension from paved roads
501   for the improvement of CALIOPE air quality system in Spain. Atmospheric Environment, 45(3), 802-
502   807. https://doi.org/10.1016/j.atmosenv.2010.10.032
503 Praticò, F.G. and Vaiana, R., 2015. A study on the relationship between mean texture depth and mean profile
504   depth of asphalt pavements. Construction and Building Materials 101 (Part 1), 72-79.
505   https://doi.org/10.1016/j.conbuildmat.2015.10.021
506 Räisänen M, Kupiainen K, Tervahattu H., 2005. The effect of mineralogy, texture and mechanical properties
507   of anti-skid and asphalt aggregates on urban dust, stages II and III. Bulletin of Engineering Geology
508   and the Environment 64, 247-256.
509 Schaap, M., Manders, A.M.M., Hendriks, E.C.J., Cnossen, J.M., Segers, A.J.S., Denier van der Gon, H.A.C.,
510   Jozwicka, M., Sauter, F.J., Velders, G.J.M., Matthijsen, J., Builtjes, P.J.H., 2009. Regional Modeling
511   of Particulate Matter for the Netherlands. http://www.rivm.nl/bibliotheek/rapporten/500099008.pdf
512   (accessed July 06, 2017).
513 Thorpe, A., Harrison, R.M., 2008. Sources and properties of non-exhaust particulate matter from road traffic:
514   A review. Science of the Total Environment 400, 270–282.
515   https://doi.org/10.1016/j.scitotenv.2008.06.007
516 Todeschini, R., 1998. Introduzione alla chemiometria. Naples, EdiSES s.r.l. (in Italian)
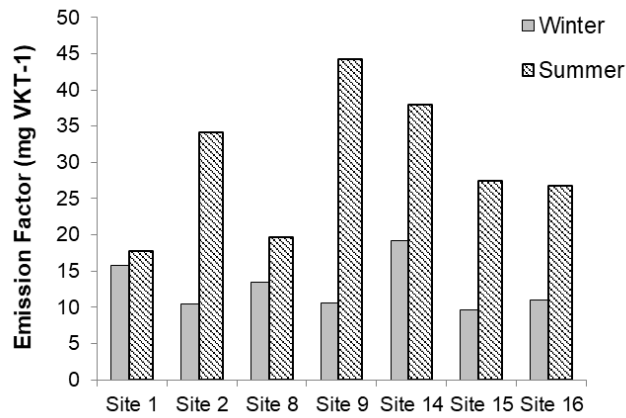517
518

519

520

521

522
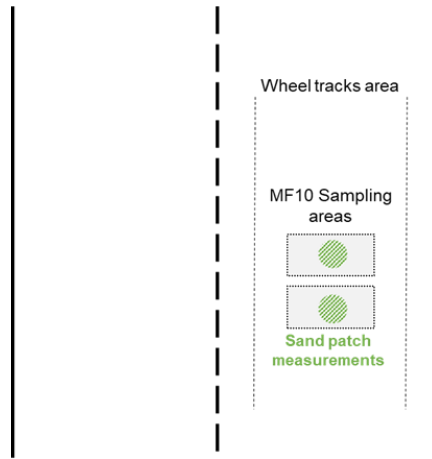
Figure 1. Placement of the sampling area within the road.

523

524

525

526

527

Figure 2. Comparison of summer and winter emission factors at selected Turin sites (where sampling was
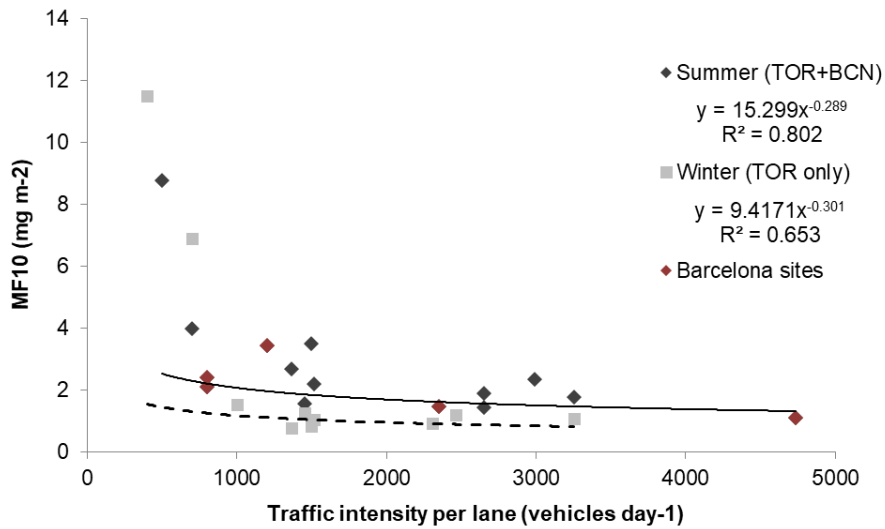made at the same spot in both seasons).
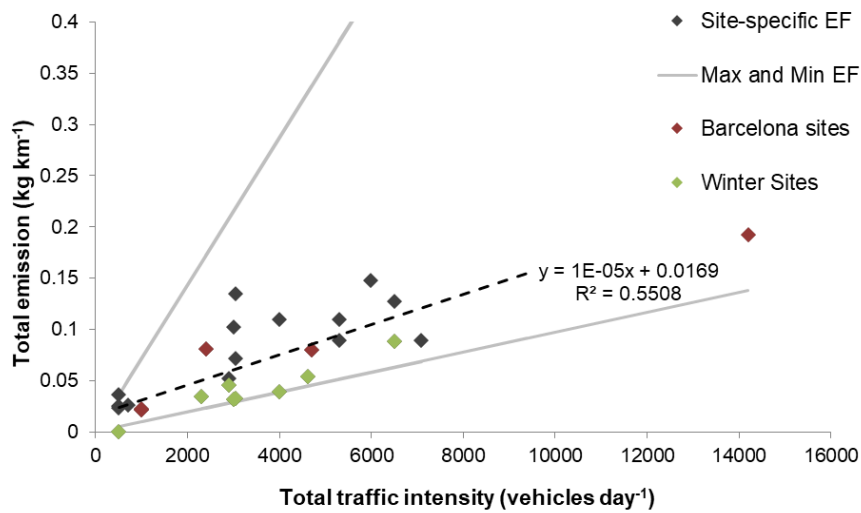
528
529

530

531

532

533

534

535   Figure 3. Relationship between MF10 and traffic intensity per lane. All sites with available traffic intensity
536   data were used. Red points belong to Barcelona sites.

537

538

539   Figure 4. Site-specific relationship between total emission per km and traffic intensity (using data of both
540   cities). Grey line represents the interval generated using the maximum and the minimum value of EFs. The
541   site with the higher traffic intensity (in red) was excluded from the fit, although in line with other samples.
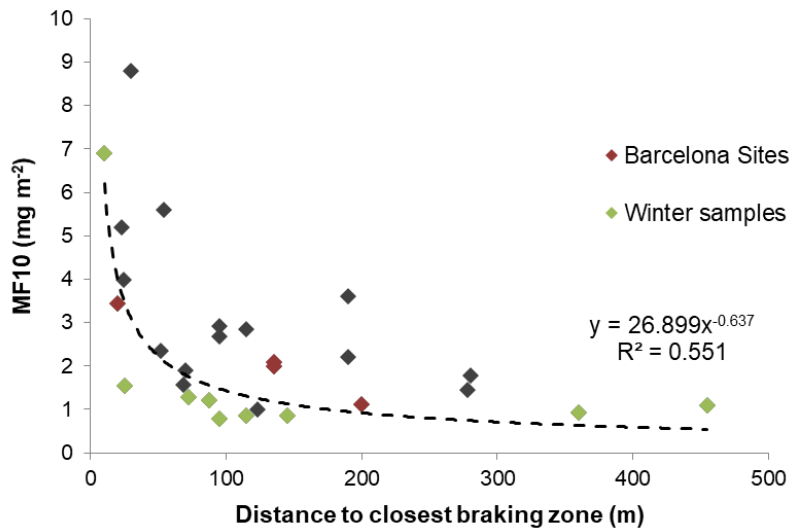542   Samples in red are of Barcelona sites, while green samples belong to winter sampling.

543

544

545

546

16

547

548   Figure 5. Relationship between MF10 and the distance from the closest braking point: stop, traffic light or

549   roundabout (using data of both cities). Samples in red are of Barcelona sites, while green samples belong to

550   winter sampling.

551
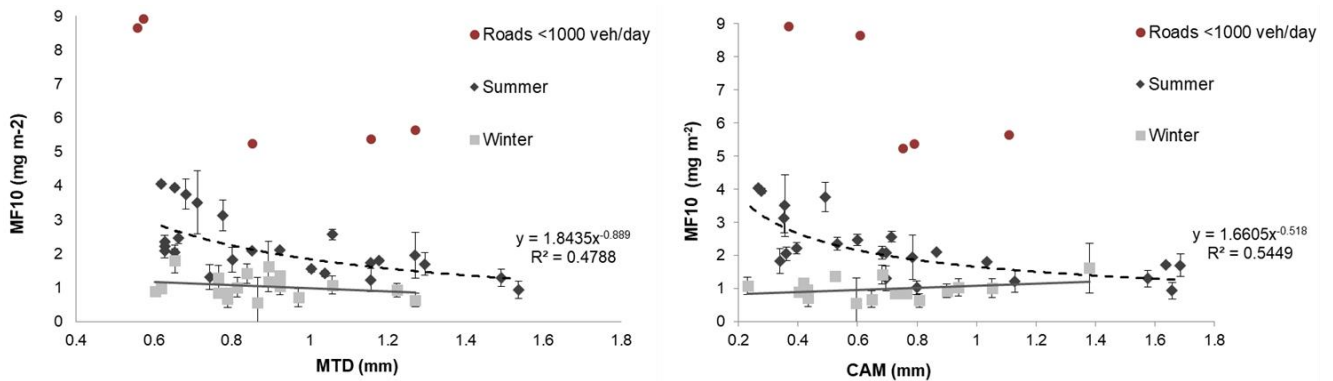
552

553   Figure 6. Relationship between MF10 and MTD (left) and CAM (right) of aggregates. All samples have been

554   used; red dots belong to sites where traffic intensity was below 1000 vehicles day[-1], and have been excluded

555   from calculations.

556

557

558

17

$y = 0.7223x + 0.5669$
$R^2 = 0.74$

559
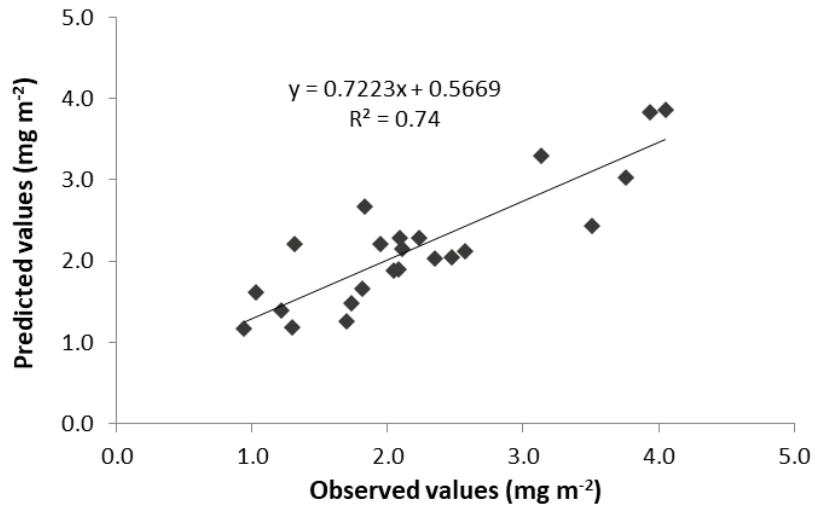
Figure 7. Observed versus predicted MF10 values, calculated using the linear regression presented in equation 3. Sites where traffic intensity was below 1000 vehicles day[-1] have been excluded from the calculations.

563

564

Table 1. Site description, pavement MTDs, MF10 loadings and calculated emission factors for each sample (average of 2 filters).

* indicates traffic values estimated with mobility models.

Season	Site number (city)	Distance from closest braking zone [m]	N° vehicles per lane [veh day^{-1}]*	Average speed (km/h)	MTD ± S.D (mm)	MF10 ± S.D. (mg m^{-2})	EF ± S.D. (mg VKT^{-1})	Notes
Summer	1S (Turin)	68	1454	38.6	0.77±0.04	1.6±0.4	18±5	
	2S (Turin)	340	1500	25.5	0.68±0.05	3.5±0.5	34±6	
	3 (Turin)	103	500*	-	0.57±0.01	8.8±0.2	72±2	
	4 (Turin)	95	15367	36.9	-	2.9±1.0	36±13	
	5 (Turin)	52	2993	30.1	0.65±0.03	2.3±0.2	25±2	
	6 (Turin)	278	2651	-	1.23±0.12	1.5±0.3	17±4	
	7 (Turin)	280	2651	-	0.62±0.04	1.8±0.2	20±2	
	8S (Turin)	70	3255	-	1.17±0.1	1.9±0.1	21±1	
	9S (Turin)	210	1519	29.6	-	3.6±0.6	44±7	
	10 (Turin)	210	1519	-	0.63±0.02	2.2±0.2	24±2	
	11 (Turin)	123	3542	32.2	0.97±0.03	1.0±0.2	13±2	
	12 (Turin)	54	500*	-	1.27±0.04	5.6±0.5	50±6	
	13 (Turin)	23	500*	-	0.85±0.02	5.2±0.4	47±5	
	14S (Turin)	25	700*	-	0.64±0.03	4.0±0.1	38±1	
	15S (Turin)	155	1367	-	1.28±0.27	2.7±0.2	27±2	
	16S (Turin)	150	1000	-	-	2.2±0.2	27±3	

	17 (Turin)	-	-	-	-	5.5±0.8	68±10	University campus road
	18 (Turin)	-	-	-	-	12.3±1.6	152±20	Park road
	19 (Turin)	70	4700	-	-	42.7±5	528±62	Construction works nearby
	20 (Barcelona)	5	1200	-	0.73±0.08	3.4±0.4	34±5	
	21 (Barcelona)	80	2350	-	1.0±0.04	1.5±0.1	17±1	
	22 (Barcelona)	65	800	-	0.89±0.07	2.0±0.01	23±1	
	23 (Barcelona)	65	800	-	1.27±0.04	2.1±0.7	21±10	
	24 (Barcelona)	200	4733	-	1.52±0.08	1.1±0.2	14±3	
	25 (Barcelona)	95	-	-	0.40±0.05	1.1±0.2	13±3	
Winter	1W (Turin)	72	1454	38.6	0.91±0.07	1.3±0.1	16±2	
	2W (Turin)	340	1500	25.5	0.78±0.04	0.85±0	11±0	
	8W (Turin)	455	3255	-	0.88±0.07	1.1±0.6	14±9	
	9W (Turin)	260	1519	29.6	0.86±0.13	0.9±0.3	11±3	
	14W (Turin)	45	500*	-	0.71±0.07	1.6±0.4	19±4	
	15W (Turin)	155	1367	-	1.25±0.05	0.8±0.2	10±3	
	16W (Turin)	150	1000	-	1.02±0.10	0.9±0.3	11±3	
	26 (Turin)	130	500*	-	-	11.5±4.5	142±55	Construction works nearby
	27 (Turin)	93	500*	-	1.03±0.16	6.9±2.2	85±27	
	28 (Turin	170	2464	14.7	0.83±0.03	1.2±0.3	15±4	
	29 (Turin)	1000	2311	23.1	0.61±0.04	0.9±0.1	12±1	